

Parity anomaly laser

Daria A. Smirnova,^{1,2} Pramod Padmanabhan,³ and Daniel Leykam³

¹*Nonlinear Physics Center, Australian National University, Canberra ACT 2601, Australia*

²*Institute of Applied Physics, Russian Academy of Sciences, Nizhny Novgorod 603950, Russia*

³*Center for Theoretical Physics of Complex Systems,
Institute for Basic Science (IBS), Daejeon 34126, Republic of Korea*

We propose a novel supersymmetry-inspired scheme for achieving disorder-robust single mode lasing in arrays of coupled microcavities, based on factorizing a given array Hamiltonian into its “supercharge” partner array. Pumping a single sublattice of the partner array preferentially induces lasing of an unpaired zero mode. Similar to 1D topological arrays, the zero mode is protected against coupling disorder. On the other hand, it need not be localized to domain walls or edges; it can be designed to have a uniform intensity profile, maximizing mode competition.

The “parity anomaly” refers to unpaired, symmetry-breaking zero modes, appearing in systems with supersymmetry (SUSY) such as strained honeycomb lattices [1–3]. A few recent studies proposed high power single mode lasing based on these anomalous zero modes: Schomerus and Halpern analyzed a parity symmetry-breaking pump in a strained honeycomb lattice [3]: the parity-breaking zero mode overlaps most strongly with the pump, resulting in a lower lasing threshold compared to the other parity-preserving modes. Hokmabadi et al. exploited mode pairing via SUSY [4–8], weakly coupling two SUSY partner lattices together and pumping one of them to achieve lasing in the zero mode. Finally, lasing in 1D arrays with topologically protected midgap states has been observed in a few recent experiments [9–14], where again pumping one of the subsystems (sublattices in this case) induces single mode lasing robust against coupling disorder. While these examples may seem unrelated, they are all ultimately mediated by the parity anomaly.

A limitation of the strained lattice and topological midgap mode proposals is that they are based on large lattices described by band structures. For integrated laser applications, small arrays of several to dozens of individual elements are preferable because slow dynamical instabilities typically inhibit synchronization of larger arrays [15, 16]. Furthermore, lasing based on localized topological zero modes is not compatible with large mode volumes, suffering from mode competition when realistic (saturable) gain is taken into account [17]. While the SUSY approach by Hokmabadi et al. is compatible with small arrays, the coupling between the two subsystems breaks the exact SUSY, introducing the additional problem of how to optimally couple the two subsystems [8]. What is needed is a way to systematically apply the parity anomaly to small systems of coupled lasers.

Here we propose a general SUSY-inspired method create unpaired zero modes for robust single mode lasing in arrays of coupled resonators. We demonstrate numerically improved performance of the resulting “parity anomaly laser” compared to topological edge mode-based lasers. In particular, in our approach the lasing mode is

not localized, so it not only harness the gain most efficiently, but mode competition is also maximized, suppressing the onset of multimode lasing.

We consider an array of M coupled resonators described by a Hermitian coupled mode Hamiltonian H_A with a non-degenerate ground state at frequency ω_0 . $H_A - \omega_0 + \epsilon$ is a positive definite Hermitian matrix for $\epsilon > 0$ and can be uniquely factorized via the Cholesky decomposition, $H_A - \omega_0 + \epsilon = L^\dagger L$, where L is a lower triangular matrix with positive real diagonal elements. This factorization of H_A allows the introduction of SUSY via the supercharge operators

$$q = \begin{pmatrix} 0 & 0 \\ L & 0 \end{pmatrix}, \quad q^\dagger = \begin{pmatrix} 0 & L^\dagger \\ 0 & 0 \end{pmatrix}, \quad (1)$$

satisfying $q^2 = (q^\dagger)^2 = 0$. The SUSY Hamiltonian $\mathcal{H} = \{q, q^\dagger\}$ commutes with the supercharge, $[\mathcal{H}, q] = [\mathcal{H}, q^\dagger] = 0$ and is block diagonal: $\mathcal{H} = \text{diag}(L^\dagger L, LL^\dagger) = \text{diag}(H_A - \omega_0 + \epsilon, H_B)$, where $H_B = LL^\dagger$ is the superpartner. In other words, $H_{A,B}$ form two decoupled systems, related by SUSY. If $\epsilon \neq 0$, SUSY is spontaneously broken: the two blocks share exactly the same eigenvalues. In the limit $\epsilon \rightarrow 0$, $H_A - \omega_0$ has an unpaired zero mode (i.e. H_B does not have a partner zero mode) and SUSY is unbroken [4, 18–21].

Previously, Refs. [5–7] suppressed multimode lasing by coupling the two blocks $H_{A,B}$ together with strength κ and pumping only H_A , such that all excited states experience weaker gain due to their hybridization with H_B . However, this is only effective for weak $\kappa \lesssim \omega_1 - \omega_0$, where ω_1 is the energy of the first excited state, since \mathcal{H} no longer commutes with the supercharge q .

Ref. [22] recently introduced a variation to this standard SUSY construction: since $q^2 = (q^\dagger)^2 = 0$, \mathcal{H} can equivalently be expressed as the square of a Dirac-like Hamiltonian $H_D = q + q^\dagger = \sqrt{\mathcal{H}}$. This new “supercharge” Hamiltonian H_D describes a single array divided into two sublattices in which there is no direct coupling between sites belonging to the same sublattice, resulting in a chiral symmetry: for every mode with energy ω , there is a partner with energy $-\omega$. This relation between

SUSY in Schrödinger and Dirac Hamiltonians has been studied for 30 years [23–25], but it has been applied to obtain topologically nontrivial lattice Hamiltonians only in the past year [22, 26–28].

When SUSY is unbroken, H_D has an unpaired zero mode exhibiting the parity anomaly: it spontaneously breaks the sublattice symmetry. This unpaired zero mode can also be explained as a topologically-protected zero mode, protected by the chiral symmetry of H_D ; the unpaired mode resides on the “majority” sublattice. Hence, by pumping the majority sublattice one can achieve robust single mode lasing. Crucially, this property is guaranteed regardless of the details of the parent lattice Hamiltonian H_A ; it is not limited to periodic lattices [9, 11–14, 26, 27], and therefore one can optimize H_A to improve the lasing performance of H_D . In particular, the topological mid-gap states of Refs. [11–13] are localized, such that the gain saturation inevitably leads to multimode lasing. With our approach, we can design delocalized unpaired zero modes with a uniform intensity distribution, maximizing the mode competition and suppressing the onset of multimode lasing.

The simplest example of a delocalized unpaired zero mode can be obtained from a ring of M identical resonators, described by the parent Hamiltonian

$$H_A = \sum_{j=1}^M (\hat{e}_{j+1,j} + \hat{e}_{j,j+1}), \quad j + M \equiv j \quad (2)$$

where matrices $\hat{e}_{j,k}$ describe coupling from site k to j (coupling strength J normalized to 1) and satisfy $\hat{e}_{j,k} \times \hat{e}_{p,q} = \delta_{k,p} \hat{e}_{j,q}$. Since H_A has a discrete rotational symmetry, all its modes have a uniform intensity distribution. This, however, means that under uniform pumping all modes will experience the same gain, inhibiting single mode lasing.

The Cholesky decomposition of H_A is (for even M)

$$L = \sum_{j=1}^{M-2} \left(\sqrt{\frac{j+1}{j}} \hat{e}_{j,j} + \sqrt{\frac{j}{j+1}} \hat{e}_{j+1,j} + \frac{(-1)^{j+1}}{\sqrt{j(j+1)}} \hat{e}_{M,j} \right) + \sqrt{\frac{M}{M-1}} (\hat{e}_{M,M-1} + \hat{e}_{M-1,M-1}), \quad (3)$$

from which the supercharge Hamiltonian $H_D = q + q^\dagger$ can be constructed using (1). Formally H_D has $2M$ sites, but the zero M th column of L implies one of the sites is completely decoupled from all others, leaving the zero mode in the $2M - 1$ coupled sites unpaired.

Fig. 1(a) illustrates the resulting SUSY and supercharge Hamiltonians. For $M > 4$ the SUSY partner H_B has a complicated structure including nonuniform and nonlocal couplings between all sites, while the supercharge Hamiltonian only requires local couplings. The site-dependent coupling strengths in (3) mean that the rotational symmetry of the parent Hamiltonian is broken

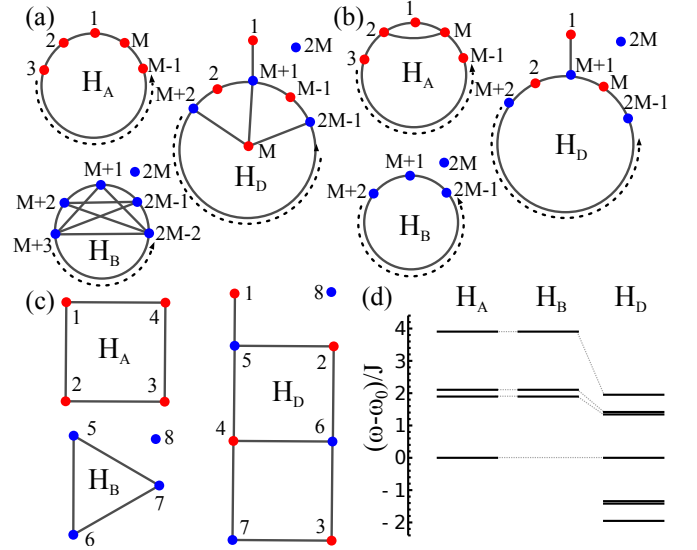


FIG. 1. Various SUSY partner Hamiltonians $H_{A,B}$ and their supercharge Hamiltonian H_D . (a) An M site ring H_A . H_B has nonlocal couplings, while H_D is a locally-coupled ring with a central “hub” site (M). (b) Generic locally-coupled H_D hosting a uniform intensity zero mode on its majority (red) sublattice. (c) $M = 4$ ring H_A , generating locally-coupled $H_{B,D}$. (d) Energy spectra of the Hamiltonians in (d). The unpaired ground state of H_A corresponds to the sublattice symmetry-breaking midgap state of H_D .

in H_D , but still all modes have their intensity uniformly distributed over the majority sublattice, and in particular the zero mode is perfectly localized to the majority sublattice with mode profile $\phi_j = (-1)^j / \sqrt{M}$.

(2) is not the only parent Hamiltonian supporting a uniform unpaired zero mode. More generally any L that annihilates ϕ is sufficient. For example, if we assume only nearest neighbor couplings are nonzero, the most general form of L supporting a uniform unpaired zero mode is

$$L = \kappa_1 \hat{e}_{2,1} + \kappa_2 \hat{e}_{N,1} + \kappa_3 \hat{e}_{1,1} + \sum_{j=2}^{M-2} c_j (\hat{e}_{j,j} + \hat{e}_{j+1,j}), \quad (4)$$

where $\kappa_3 = \kappa_1 + (-1)^M \kappa_2$ and other couplings c_j and $\kappa_{1,2}$ are free parameters. The resulting SUSY and supercharge networks are illustrated in Fig. 1(b). Here the uniform intensity is enabled by the paired coupling terms c_j , while the additional defect site side-coupled by κ_1 allows the zero mode to be unpaired. Interestingly, in this case the SUSY Hamiltonians $H_{A,B}$ both form closed rings with local couplings, and the zero mode of H_A has a uniform intensity despite the couplings, site detunings, and excited states all being inhomogeneous.

To demonstrate the potential of such unpaired zero modes for arrays of small coupled lasers, we now study in detail the supercharge array generated by the $M = 4$ ring of (2). Fig. 1(c,d) illustrates H_A , its partner Hamiltonian

ans H_B and H_D , and their corresponding energy spectra. In particular, the spectrum of H_D is compressed (with normalized eigenvalues $\omega_n/J \rightarrow \sqrt{\omega_n/J}$, increasing the detuning between the zero mode and first excited state [22].

Next, we introduce gain and loss to the supercharge Hamiltonian H_D to describe a coupled laser array. We assume that only the majority lattice (hosting the unpaired zero mode) is pumped (inducing gain g), while the minority sublattice has fixed loss γ . Close to the lasing threshold, where light intensities are low and gain saturation effects can be neglected, the emission spectrum under pulsed optical pumping is determined by the eigenvalues of the linear Hamiltonian $H_D + i\text{diag}(g, g, g, g, -\gamma, -\gamma, -\gamma)$. In particular, lasing can occur in all modes whose eigenvalues have a positive imaginary part.

Fig. 2(a,b) plots the energy eigenvalues of the array as a function of the gain g for fixed loss $\gamma = J$. We observe behavior very similar to the recently demonstrated 1D topological laser arrays [11–13]: the zero mode shown in Fig. 2(c) most efficiently harnesses the gain ($\text{Im}(\omega_0) = g$) and its threshold is independent of the loss on the minority sublattice, since it is perfectly localized to the majority sublattice. The other modes [see e.g. Fig. 2(d,e)] initially have their power equally distributed between the majority and minority sublattices, reducing their slope efficiency and inducing a γ -dependent threshold. At a critical gain-loss imbalance, each mode undergoes a parity-time symmetry (PT)-breaking transition and begins to localize to the pumped sites, such that it competes more strongly with the zero mode.

In contrast to the 1D topological laser arrays, here the zero mode uniformly excites all the pumped sites, so it can saturate the gain and maintain single mode operation over a wider range of parameters. To describe the gain saturation we consider a class B laser model describing coupled resonators with embedded InGaAsP quantum wells [13, 15, 16],

$$i\partial_t\psi_n = (H_D + H_P)\psi_n, \quad (5a)$$

$$H_P\psi_n = \frac{1}{2} \left(-\frac{1}{\tau_p} + \sigma(N_n - 1) \right) (i - \alpha)\psi_n, \quad (5b)$$

$$\partial_t N_n = R_n - \frac{N_n}{\tau_r} - \frac{2}{\tau_r} (N_n - 1)|\psi_n|^2, \quad (5c)$$

where ψ_n and N_n are the field amplitude and carrier density at the n th site, τ_p is the photon cavity lifetime, σ is proportional to the differential gain, α is the linewidth enhancement factor, R_n is the normalized (site-dependent) pumping rate, and τ_r is the carrier lifetime. For our numerical simulations, we take values representative of the pumped microring resonators in considered in Refs. [13, 15]: $\tau_p = 40$ ps, $\tau_s = 100\tau_p$, $\sigma = 24/\tau_p$, $J = 3/\tau_p$, and $\alpha = 3$, and assume the majority and minority sublattices are pumped with strength R_A and R_B

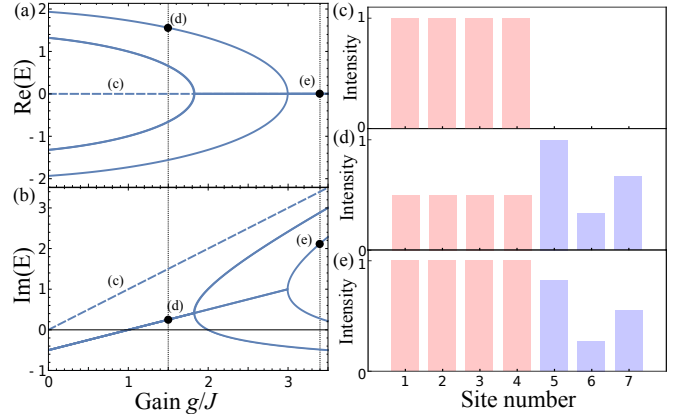


FIG. 2. Spectrum of H_D when the majority sublattice is pumped with strength g , while minority sublattice has fixed loss $\gamma = J$. (a,b) Real and imaginary parts of eigenvalues. As the gain is increased the excited states coalesce at $\text{Re}(\omega) = 0$ in a PT-breaking transition. (c) Unpaired zero mode profile [dashed lines in (a,b)]. (d) Representative excited state mode profile below the PT-breaking transition ($g/J = 1.5$). Its power is distributed equally between the majority (red) and minority (blue) sublattices. (e) Excited state mode profile above the PT-breaking transition ($g/J = 3.4$). It localizes more strongly on the majority sublattice, leading to stronger mode competition.

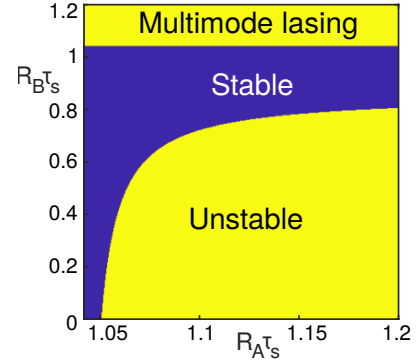


FIG. 3. Stability diagram of the unpaired zero mode as a function of the majority (R_A) and minority (R_B) sublattice pump strengths. The lower limit of R_A is the lasing threshold.

respectively.

The lasing intensity of the zero mode, $I_0 = \frac{1}{2}((R_A\tau_s - 1)\tau_p\sigma - 1)$, is obtained from (5) by assuming it saturates the gain at the majority sites. It is identical to that of a single ring, being independent of the energy scale J set by the inter-site couplings and the pump rate on the minority sublattice. Nevertheless, its stability is sensitive to these parameters. We perform the linear stability analysis by linearizing (5) about the zero mode solution (see e.g. Ref. [16]).

Fig. 3 plots the stability as a function of the two pump rates $R_{A,B}$, revealing a large parametric domain of single mode lasing. When the minority pump rate R_B is low, the effective coupling between the pumped sites is

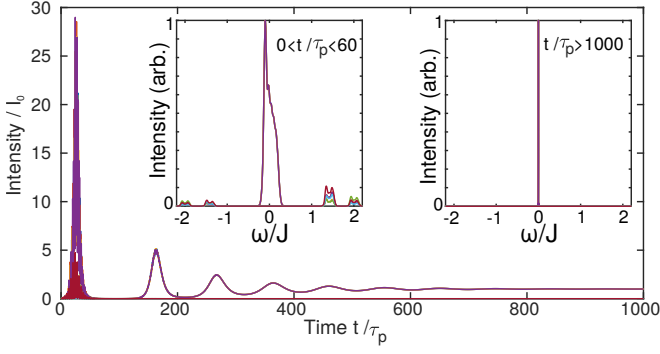


FIG. 4. Switch-on dynamics of the laser, revealing suppression of all excited states due to gain saturation and stable lasing in the unpaired zero mode. Insets show Fourier spectra during (left) and after (right) the initial transient.

weak due to the high losses in the minority sites. In this weakly-coupled regime, when the zero mode first becomes unstable the system converges to a stable asymmetric mode, predominantly localized to the majority sublattice. At even stronger pump rates, this asymmetric mode first undergoes a Hopf bifurcation into a limit cycle, before emergence of chaotic dynamics [29]. Meanwhile, the upper multimode lasing region in Fig. 3 corresponds to the pump R_B exceeding the losses at the minority sites. In this strongly-coupled regime, lasing occurs at multiple frequencies with splitting determined by the inter-site coupling strength J .

To validate the above linear stability analysis, we also performed direct time-domain simulations of (5) starting from random noise in the optical field ψ_n and equilibrium carrier densities $N_n(0) = R_n \tau_s$. We assume pump rates identical to those used in the recent experiments of Ref. [13]: $R_A = 1.07/\tau_s$ (above threshold) and $R_B = 1.03/\tau_s$ (slightly below threshold). This corresponds to initial (small signal) gain and loss rates of $g \approx 0.07J$ and $\gamma \approx g/10$ respectively, such that all linear modes are initially above the lasing threshold.

Fig. 4 illustrates the resulting dynamics. Initially all linear modes are above threshold and start to grow, such that the emission spectrum measured under pulsed optical pumping would reveal multiple peaks corresponding to the linear modes of H_D (see left inset in Fig. 4). At longer times, however (e.g., under continuous electrical pumping), the gain saturation plays a critical role. The zero mode grows the fastest, and since it uniformly excites all pumped sites it is able to completely saturate the gain and suppress all other modes. Thus, after an initial transient the system converges to the stable unpaired zero mode lasing state.

To demonstrate the importance of the uniform mode profile in achieving the stable single mode lasing, Fig. 5 compares the performance of a parity anomaly laser model generated from an *open* chain. In this case, the parent Hamiltonian lacks any discrete rotational symme-

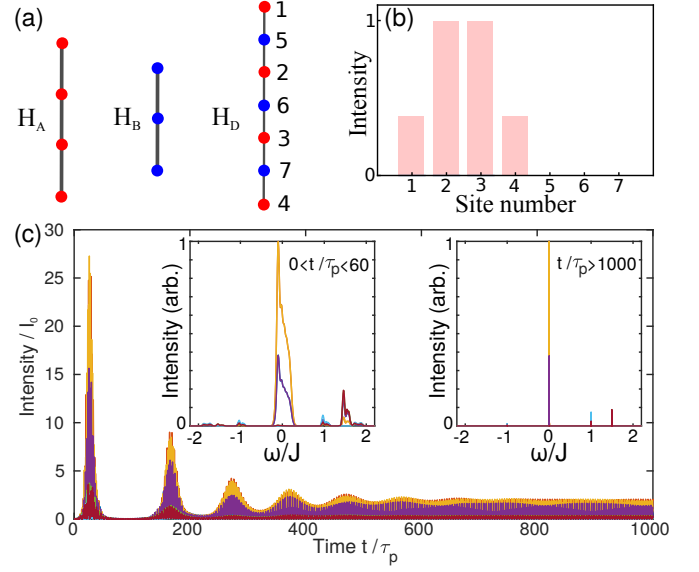


FIG. 5. Parity anomaly laser derived from a 1D chain. (a) $M = 4$ site chain, its SUSY partner H_B , and corresponding supercharge Hamiltonian H_D . (b) Unpaired zero mode, exhibiting a non-uniform intensity on majority sublattice. (c) Laser switch-on dynamics, revealing persistent multimode lasing because the zero mode cannot saturate the gain. Insets: Fourier spectra during (left) and after (right) initial transient.

try and the zero mode does not uniformly excite all the pumped sites (similar to the case of the 1D topological edge state lasers). Consequently, the zero mode cannot saturate the gain by itself and lasing in excited states persists, resulting in persistent multimode emission.

Before closing, we briefly comment on the robustness of this parity anomaly laser to imperfections. The unpaired zero mode is protected by the bipartite symmetry of the network - its division into minority and majority sublattices. It is therefore robust against perturbations to the coupling strengths, similar to the familiar SSH chain [9, 11–14]. We checked that the stability diagram and switch-on dynamics are both insensitive to moderate coupling disorder, which does not affect the frequency of the zero mode but only modulates its intensity profile.

In summary, we propose a supersymmetry-inspired method to achieve stable single mode lasing in coupled microcavity networks, based on unpaired zero modes occurring in “supercharge” resonator networks [22]. The advantage of our scheme is that the symmetry-protected zero mode is not localized and is therefore able to completely saturate the gain, preserving single mode operation above the thresholds observed in Refs. [11–13]. An interesting future direction would be to generalize this scheme to genuinely two-dimensional arrays [30–32].

This work was supported by the Institute for Basic Science in Korea (IBS-R024-Y1) and the Russian Foundation for Basic Research (Grant 18-02-00381). We thank Vassilios Kovanis and Sunkyu Yu for enlightening discus-

sions.

-
- [1] G. W. Semenoff, Phys. Rev. Lett. **53**, 2449 (1984).
 - [2] F. D. M. Haldane, Phys. Rev. Lett. **61**, 2015 (1988).
 - [3] H. Schomerus and N. Y. Halpern, Phys. Rev. Lett. **110**, 013903 (2013).
 - [4] M.-A. Miri, M. Heinrich, R. El-Ganainy, and D. N. Christodoulides, Phys. Rev. Lett. **110**, 233902 (2013).
 - [5] R. El-Ganainy, L. Ge, M. Khajavikhan, and D. N. Christodoulides, Phys. Rev. A **92**, 033818 (2015).
 - [6] M. H. Teimourpour, L. Ge, D. N. Christodoulides, and R. El-Ganainy, Scientific Rep. **6**, 33253 (2016).
 - [7] M. P. Hokmabadi, S. Faryadras, R. El-Ganainy, D. N. Christodoulides, and M. Khajavikhan, CLEO 2018 FM4E.7 (2018).
 - [8] W. Walasik, B. Midya, L. Feng, and N. M. Litchinitser, Opt. Lett. **43**, 3758 (2018).
 - [9] H. Schomerus, Opt. Lett. **38**, 1912 (2013).
 - [10] L. Polozzi and C. Conti, Phys. Rev. B **93**, 195317 (2016).
 - [11] P. St-Jean, V. Goblot, E. Galopin, A. Lemaitre, T. Ozawa, L. Le Gratiet, I. Sagnes, J. Bloch, and A. Amo, Nature Photon. **11**, 651 (2017).
 - [12] H. Zhao, P. Miao, M.H. Teimourpour, S. Malzard, R. El-Ganainy, H. Schomerus, and L. Feng, Nature Commun. **9**, 981 (2017).
 - [13] M. Parto, S. Wittek, H. Hodaei, G. Harari, M.A. Bandres, J. Ren, M.C. Rechtsman, M. Segev, D.N. Christodoulides, and M. Khajavikhan, Phys. Rev. Lett. **120**, 113901 (2018).
 - [14] S. Malzard and H. Schomerus, New J. Phys. **20**, 063044 (2018).
 - [15] S. Longhi, Y. Kominis, and V. Kovanis, EPL **122**, 14004 (2018).
 - [16] S. Longhi and L. Feng, APL Photonics **3**, 060802 (2018).
 - [17] S. Longhi, Ann. Phys. **530**, 1800023 (2018).
 - [18] E. Witten, Nucl. Phys. B **188**, 513 (1981).
 - [19] M.-A. Miri, M. Heinrich, and D. N. Christodoulides, Optica **1**, 89, (2014).
 - [20] S. Yu, X. Piao, J. Hong, and N. Park, Nature Comms. **6**, 8269 (2015).
 - [21] Y. Nakata, Y. Urade, T. Nakanishi, F. Miyamaru, M. W. Takeda, and M. Kitano, Phys. Rev. A **93**, 043853 (2016).
 - [22] B. Midya, W. Walasik, N. M. Litchinitser, and L. Feng, Opt. Lett. **43**, 4927 (2018).
 - [23] Y. Nogami and F. M. Toyama, Phys. Rev. A **47**, 1708 (1993).
 - [24] F. Cooper, A. Khare, R. Musto, and A. Wipf, Ann. Phys. **187**, 1 (1988).
 - [25] L. M. Nieto, A. A. Pecheritsin, and B. F. Samsonov, Ann. Phys. **305**, 151 (2003).
 - [26] J. Arkinstall, H. M. Teimourpour, L. Feng, R. El-Ganainy, and H. Schomerus, Phys. Rev. B **95**, 165109 (2017).
 - [27] S. Barkhofen, L. Lorz, T. Nitsche, C. Silberhorn, and H. Schomerus, arXiv:1804.09496.
 - [28] M. Kremer, I. Petrides, E. Meyer, M. Heinrich, O. Zilberberg, and A. Szameit, arXiv:1805.05209.
 - [29] Y. Kominis, V. Kovanis, and T. Bountis, Phys. Rev. A **96**, 043836 (2017).
 - [30] B. Bahari, A. Ndao, F. Vallini, A. El Amili, Y. Fainman, and B. Kante, Science **358**, 636 (2017).
 - [31] M. A. Bandres, S. Wittek, G. Harari, M. Part, J. Ren, M. Segev, D. N. Christodoulides, M. Khajavikhan, Science **359**, eaar4005 (2018).
 - [32] G. Harari, M. A. Bandres, Y. Lumer, M. C. Rechtsman, Y. D. Chong, M. Khajavikhan, D. N. Christodoulides and M. Segev, Science **359**, eaar4003 (2018).